*Geophysical Prospecting*, 2009, **57**, 665–681 doi: 10.1111/j.1365-2478.2009.00800.x

# A discussion of structural and thermal control of magnetic anomalies on the mid-Norwegian margin

Jörg Ebbing[1,2,*], Laurent Gernigon[1], Christophe Pascal[1], Odleiv Olesen[1] and Per Terje Osmundsen[1]

[1]*Geological Survey of Norway, 7491 Trondheim, Norway, and* [2]*Department of Petroleum Engineering and Applied Geophysics, Norwegian University of Science and Technology, 7491 Trondheim, Norway*

Received February 2008, revision accepted February 2009

## ABSTRACT

We discuss the correlation between the depth extent of magnetic sources, the Curie temperature depth and crustal structures on the mid-Norwegian margin. Spectral methods can be used to estimate the depth extent of magnetic sources, even if the bottom is located in the lower crust, however, only with limited resolution. The bottom of the magnetic surfaces is often regarded to represent the depth to the Curie isotherm. However, comparison with a 3D model based on the interpretation of potential field and seismic reflection data and thermal modelling shows that the depth extent of the magnetic sources is merely controlled by the overall geometry of the crystalline crust and not the temperature distribution. The observed changes in the magnetic field between the inner and outer part of the mid-Norwegian margin appears not to reflect, as previously assumed, the depth to the Curie temperature but the geometry of the basement and lower crust. Our 3D model of the mid-Norwegian margin reveals a basement configuration that involves a basement with different petrophysical properties, which can be connected with lithological basement units of onshore Norway.

## INTRODUCTION

Estimation of the thermal state of the lithosphere is one of the most challenging topics in Earth Sciences today. Temperature is one factor controlling lithospheric rheology (e.g., McKenzie, Jackson and Priestley 2005) but also provides information on hydrocarbon systems (e.g., Nadeau, Bjørkum and Walderhaug 2005). The latter is leading to an increased interest from the hydrocarbon industry in estimations of the thermal structure of continental margins.

The thermal state of the crust is traditionally constrained by surface heat flow data (e.g., Beardsmore and Cull 2001). In absence of good constraints on the structure of the crust and on its associated thermal parameters (i.e., thermal conductivities and distribution of radioactive heat sources), extrapolation of these (near) surface data to deeper levels into the crust can lead to large uncertainties, increasing with depth. An additional thermal boundary condition in the subsurface would, ideally, allow for better constraining the thermal structure of the crust. Estimates of the depth to the base of the lithosphere (assumed to be the ~1300°C isotherm) from independent geophysical methods or the study of mantle xenoliths can eventually furnish this missing boundary condition (e.g., Kukkonen and Peltonen 1999; Artemieva and Mooney 2001). However, the occurrence of mantle xenoliths is very rare and geophysical methods have not yet enough resolution.

The geophysical data set that is most dependent on temperature, other than heat flow itself, is the magnetic field. Rocks effectively lose their ability to maintain magnetization with temperatures higher than the Curie temperature and the magnetic field should theoretically reflect this temperature dependency (e.g., Fowler 2005). If it was possible to identify the depth to the Curie temperature from magnetic data, it would

*E-mail: joerg.ebbing@ngu.no

 

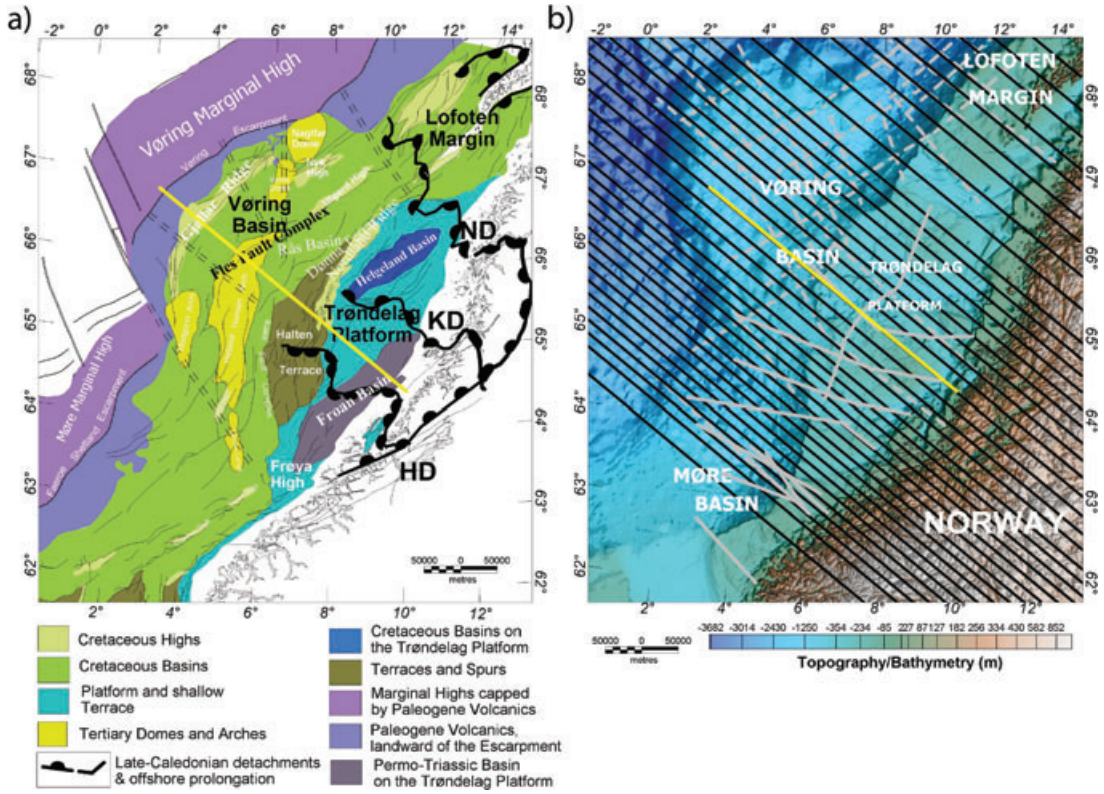


**Figure 1** a) Major structural elements of the mid-Norway rifted margin (modified from Blystad *et al.* 1995). HD: Høybakken detachment, KD: Kollstraumen detachment (shear zone), ND: Nesna detachment (Olesen *et al.* 2002; Osmundsen *et al.* 2002; Ebbing *et al.* 2006). b) Bathymetry (modified after Dehls *et al.* 2000). The yellow line shows the location of the profiles presented in Fig. 5 and grey lines show the location of OBS profiles and wide-angle reflection profiles used in building the 3D. The black lines show the set-up of the 3D model presented in this study.

be possible to give an independent and complementary constraint for the present-day thermal state. One commonly used technique for estimating the base of magnetic sources is to analyse the shape of the power spectrum of magnetic profiles or gridded data (e.g., Bhattacharyya 1964; Spector and Grant 1970a,b; Okubo *et al.* 1985; Blakely 1996). However, the question arises whether these conventional spectral techniques can provide reliable depth estimates and if these estimates represent the Curie isotherms or a structural boundary.

We discuss thermal versus structural control on the depth to the magnetic sources for the mid-Norwegian margin, located off Norway (Fig. 1). The margin comprises three main segments, the Trøndelag Platform, the Vøring Basin and the Vøring Marginal High; which are separated by N-S and NE-SW-trending fault systems (Blystad *et al.* 1995). Seismic studies and potential field studies have shown that the basins underlying the margin have a thickness up to 15 km (e.g., Brekke 2000; Skilbrei and Olesen 2005; Mjelde *et al.* 2005).

Potential field studies constrained by seismic profiles can help to identify the 3D structure of the basement underlying sedimentary basins (e.g., Skilbrei and Olesen 2005; Ebbing *et al.* 2006), which is important for models of basin evolution. Using common interpretation techniques, gravity and magnetic data can be used to constrain the top basement as well as the base of the crust (Moho) and to identify different intra-basement domains, if they are expressed by changes in petrophysical properties.

The magnetic field over the Vøring margin shows a clear distinction between low-amplitude anomalies over the Vøring Basin and high-amplitude anomalies over the Trøndelag Platform (Fig. 2). Previous studies argued that the low-amplitude anomalies at the outer margin are associated with a shallow depth to the Curie temperature due to a high geothermal gradient (e.g., 12.5 km at the continent-ocean-transition, deepening landwards to 22.5 km below the coastline; Fichler *et al.* 1999). Towards the innermost margin the Curie depth is supposed to deepen rapidly, which allows the development of the large magnetic amplitude observed over the Trøndelag Platform, while on the outer margin only the uppermost basement has a contribution to the magnetic field. Recent

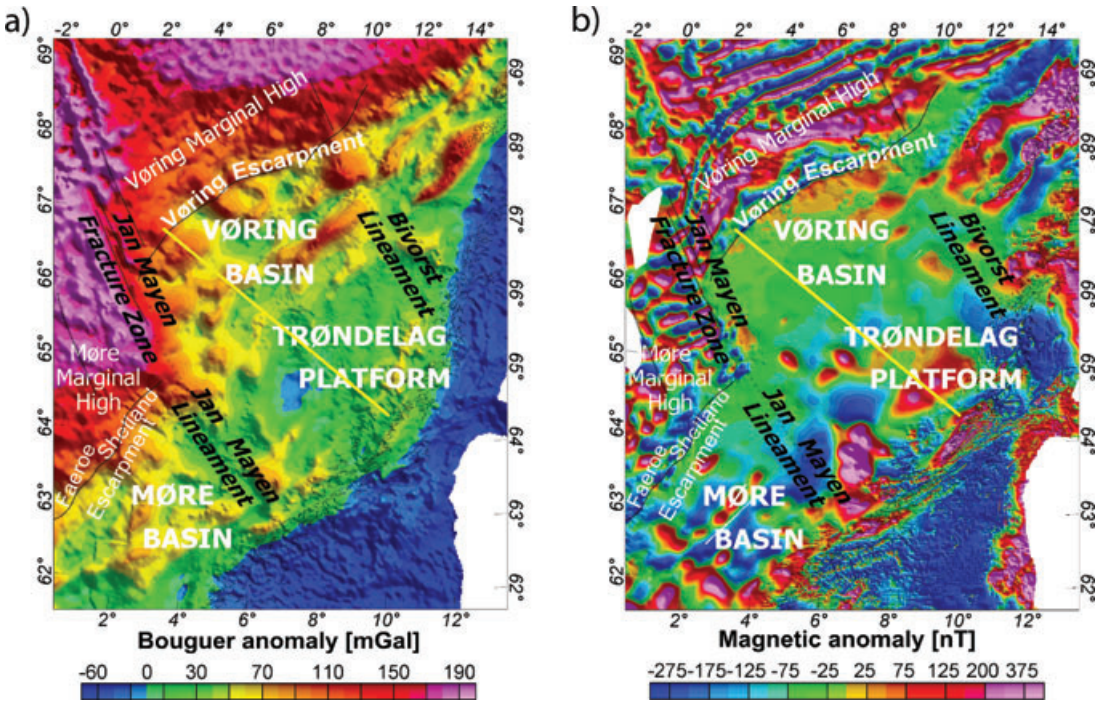


**Figure 2** a) Bouguer gravity anomaly, b) total magnetic field anomaly. a) The Bouguer anomaly is calculated with an offshore reduction density of 2.2 Mg/m$^3$. Offshore measurements of approximately 59 000 km of marine gravity profiles have been acquired by the Norwegian Petroleum Directorate, oil companies and the Norwegian Mapping Authorities. In addition, gravity data from satellite altimetry in the deep-water areas have been used (Andersen and Knudsen 1998). The surveys have been levelled using the International Standardization Net 1971 (IGSN 71) and the Gravity Formula 1980 for normal gravity (Skilbrei *et al.* 2000). b) The total magnetic field anomaly is referred to as DGRF on the mid-Norwegian continental margin. Eight offshore aeromagnetic surveys have been processed and merged to produce the displayed map (Olesen *et al.* 2007).

studies have cast some doubts on this assumption by combining structural and thermal modelling along a transect crossing the margin (Gernigon *et al.* 2004, 2006).

We discuss the source of the deepest magnetic sources by applying a combination of forward and inverse modelling techniques and discuss the thermal state by comparison with forward thermal models, which allows evaluation of Curie depth estimates under deep sedimentary basins.

## MAGNETIC ANOMALIES, PROPERTIES AND CURIE TEMPERATURE

Figure 2 presents the magnetic and gravity anomalies of the mid-Norwegian margin. The Bouguer anomaly is based on a compilation by Skilbrei *et al.* (2000) and uses IGSN as a reference network (see Fig. 2 caption for more details). The total magnetic field anomaly is a composite map of different offshore aeromagnetic surveys. Olesen *et al.* (2007) discussed the processing with different techniques in detail. The pattern of flight lines generally provides data along NW-SE trending lines with a spacing of 2–5 km (Olesen *et al.* 2007). While a number of new surveys only covers parts of the margin, surveys from the 1970s cover the entire margin (e.g., Åm *et al.* 1975). The superposition of surveys and area overlap provides a fair control on the long-wavelength as well as the short-wavelength anomalies. The magnetic field is computed using DGRF as a reference magnetic field and for the 3D forward modelling the precise angle of declination and inclination was used.

The resulting total magnetic field anomaly of the mid-Norwegian margin shows a clear difference between the innermost margin segments, the Trøndelag Platform and the outer segment, the Vøring Basin, which is not as prominent in the gravity anomalies. Over the Trøndelag Platform the magnetic anomalies show amplitudes from <–300 to >+500 nT, while the magnetic anomalies on the Vøring Basin generally vary around –50 ± 50 nT. Such a large change in the magnetic field must also be associated with large changes in the magnetic properties of the crust.

West of the Vøring escarpment the magnetic anomalies show large-scale stripe patterns, which mark the transition to the oceanic domain. Clearly, these anomalies are related to sea-floor spreading anomalies and crustal intrusions in the transition area. Olesen *et al.* (2007) and Gernigon *et al.* (2009) discussed the meaning of these anomalies in detail in terms of the early spreading history of the Norwegian-Greenland Sea.

Magnetic total field anomalies only provide information for the part of the crust and mantle that presently resides at temperatures below the Curie temperature. The Curie temperature of a ferromagnetic material is the temperature where the material looses its characteristic ferromagnetic ability: the ability to possess a net and spontaneous magnetization in the presence of an external inducing magnetic field. Rocks at higher temperatures will not generate a discernible magnetic signal. Magnetite, with a Curie temperature of 580°C (e.g., Hunt, Moskowitz and Banerje 1995), is regarded to be the dominant magnetic mineral in crustal rocks. The Curie temperatures for felsic plutonic rocks can range from 400–550°C, related to variability in composition of titanomagnetites between substantially different rock types (e.g., basalt versus granite, cf., Byerly and Stolt, 1977). The Curie temperature range also reflects the gradual loss of magnetic properties, which starts at the lowest temperature bound. In most stable continental areas this temperature range runs through the lower crust or upper mantle (e.g., McKenzie *et al.* 2005).

Changes in magnetic anomalies can be associated with the lithology of the crust and its thermal structure. The deepest boundary for magnetic sources within the crust may be governed either by a crustal interface, which could be the case in areas with relatively low crustal temperature gradients, or by the loss of magnetic properties due to temperatures higher than the Curie temperature, in areas with high temperature gradients. In the second case, the depth of the deepest magnetic source can be interpreted as the Curie isotherm (e.g., Blakely 1996).

To estimate Curie temperature depths from aeromagnetic surveys, several techniques have been applied in the past. One commonly used technique is to analyse the shape of the power spectrum of gridded data (e.g., Bhattacharyya 1964; Spector and Grant 1970a; Okubo *et al.* 1985; Blakely 1996).

## SPECTRAL ESTIMATES

Aeromagnetic anomalies are caused by an ensemble of sources. On passive margins the main sources of the magnetic field are the underlying basement and intra-sedimentary volcanic rocks. Sediments are relatively non-magnetic; while basement and intrusive rocks have high- magnetic susceptibilities (see below).

For the purpose of analysing aeromagnetic maps, the field is assumed to be the response to a number of independent sources, characterized by a joint frequency distribution in depth, width, length and direction cosines of magnetization. In theory, spectral methods allow separating the effects of each ensemble in the aeromagnetic map (e.g., Bhattacharyya 1964; Spector and Grant 1970a,b; Blakely 1996; Naidu and Mathew 1998).

Common methods to estimate the source depth are Euler deconvolution, power spectrum methods or Werner deconvolution. Especially, Euler deconvolution is widely used to provide estimates on the top basement, in particular in combination with seismic data (e.g., Olesen *et al.* 2002; Skilbrei and Olesen 2005). Spectral methods to estimate the depth extent of magnetic sources have been used in the past and various studies apply the spectral methods to define the Curie temperature (e.g.; Shuey *et al.* 1977; Connard, Couch and Gemperle 1983; Aydin, Karat and Koçak 2005; Ross, Blakely and Zoback 2006).

Figure 3(a) presents the power density spectrum obtained for a selected window, following the classical approach by Spector and Grant (1970a); see also Appendix for mathematical background. The slope of each linear segment provides information about the depth to the top of an ensemble of magnetic sources.

Okubo *et al.* (1985) presented a modification of the original spectral approach from Spector and Grant (1970) in such a way that a single prism represents an entire set of different scattered magnetic sources. In this method both the depths to the top and the centroid of the magnetic ensemble are estimated, which allows calculating the depth to the bottom of the magnetic ensemble (see Appendix for mathematical background). However, the depths to the top, to the centroid and to the bottom of the statistical prism obtained with this method may depend on the grid sample size. In particular, the sampling window must be chosen large enough to cover the main magnetic anomalies and to detect the deepest magnetic sources. The depth to the bottom of magnetic sources obtained very large windows that may correspond to the depth to the Curie temperature.

Sensitivity tests applying the Okubo *et al.* (1985) approach (Fig. 4) show that a window size of minimum 200 km × 200 km is required to study sources at 20 km depth, hence in the lower crust. In cases where the bottom of the magnetic sources is even deeper, the window size has to be even larger to resolve the long-wavelength part of the anomalies.

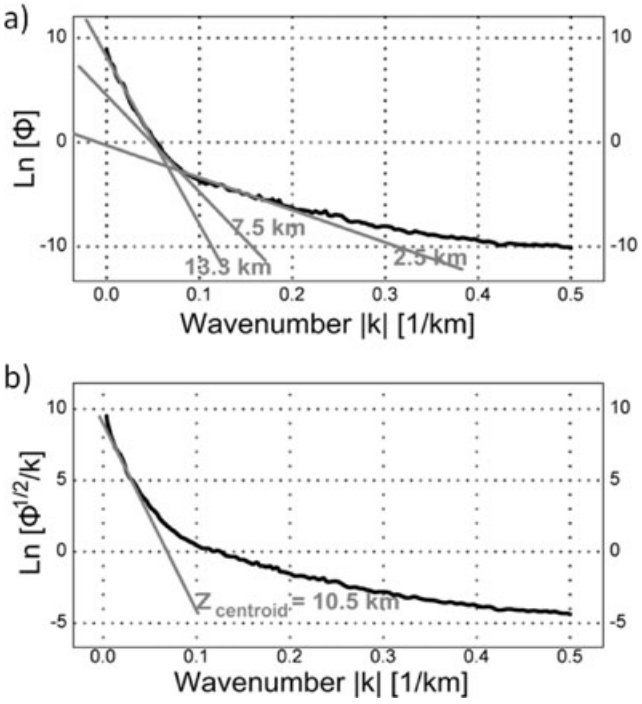


**Figure 3** Examples of radial averaged spectra for the magnetic depth estimations in the window labelled S (Fig. 4) of 250 × 250 km size. a) Radial averaged power spectra to estimate the top of the deepest magnetic source; b) radial averaged spectrum divided by the wavenumbers to estimate the centroid of the deepest magnetic source (after Okubo *et al.* 1985). From the spectra, values of 7.5 km and 10.5 km are obtained as the top bound and the centroid using the gradient of spectra defined in equations (5) and (6), respectively. Applying equation (7), we obtain 13.5 km for the base of the magnetic prism.

Simultaneously this leads to superposition of sources on the medium to short-wavelength part of the spectra, which makes the depth estimates more uncertain (Figs 3 and 4). Hence, only rough estimates for very large regions can be made with this approach.

Using small windows in the continental domain (Fig. 4), the depth estimations vary from >18 km (deeper values) at the coast to ~12 km at the ocean-continent transition and <9 km on the oceanic plate. Using larger windows leads to depth estimates that vary from ~20 km at the coast to ~17–19 km below the Vøring margin and <16 km in the oceanic domain. The depth estimates obtained through the spectrum approach indicate shallower depths of the bottom of magnetic sources beneath the outer margin than on the inner margin.

However, the variations of the depth estimates with the size of the computation window and the absence of a peak at small wavenumbers in the power spectrum of magnetic anomalies (as predicted by Spector and Grant 1970) may indicate that the window size is too small to detect the deepest magnetic sources.

In addition, several studies indicate that the Spector and Grant (1970) assumptions might not be adequate for crustal magnetization (e.g., Pilkington and Todoeschuck 1993; Maus, Gordon and Fairhead 1997; Fedi, Quarta and De Santis 1997). For instance, Fedi *et al.* (1997) suggested that the power spectra should be corrected for a power law decay before depth estimation. The spectral method also assumes a random distribution of magnetized bodies, which is clearly not the case in the oceanic domain where linear magnetic anomalies can be observed (Figs 2b and 4). Due to the required large window size, it is not possible to exclude magnetic anomalies from the oceanic domain. For all these reasons, it is not straight forward that the spectral method used in this study is applicable in the mid-Norwegian margin and depth estimates should be used with caution. In particular, absolute values of the results may be biased and affected by very large uncertainties, while relative variations of the depth to the bottom of magnetic sources might be reliable.

The nature of the bottom of magnetic sources is also uncertain and our observations can be explained by variations of Curie temperature depths, or variations of the depth and geometry of a lithological interface. To identify the geological meaning of our depth estimates on the continental margin, we compare them in the remainder to a 3D model of the density and magnetic properties distribution constrained by seismic data and 2D thermal modelling.

## FORWARD MODELLING

The mid-Norwegian margin has been extensively studied by means of multi-channel seismic reflection data, seismic refraction data and commercial and scientific drilling. Together with results from previous studies (e.g., Skogseid *et al.* 1992; Doré *et al.* 1999; Brekke 2000; Mjelde *et al.* 2001; Raum *et al.* 2002; Mjelde *et al.* 2003a,b), new interpretation of long-offset reflection data (Osmundsen and Ebbing 2008) and ocean-bottom seismometer (OBS) lines (e.g., Mjelde *et al.* 2005, 2008) allow us to model the detailed 3D crustal geometry of the margin in the Vøring and Møre basins and in the Trøndelag Platform area.

The 3D geometry of the model has been tested against gravity and magnetic fields. The gravity and magnetic anomalies generally contain different wavelengths due to their contrasting dependencies on the distance to the source $r$, e.g., for a point mass the gravity field falls off with $1/r^2$, while the magnetic field falls off with $1/r^3$. The stronger dependency on the

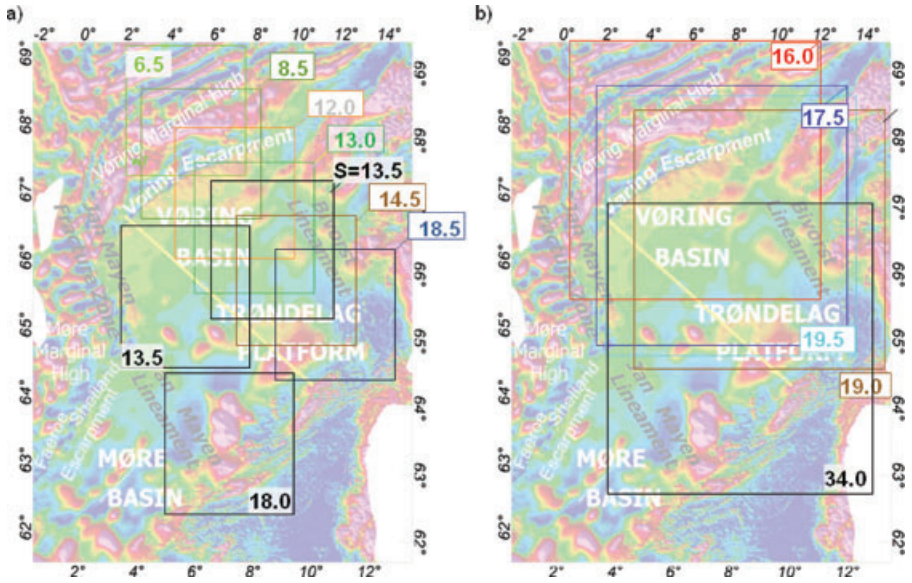


**Figure 4** Results of estimates of base of magnetic sources by the spectral approach and selected windows along a NW-SE corridor from the Norwegian mainland to oceanic spreading axes. a) Window size is 250 × 250 km; b) window size is 475 × 475 km. See Fig. 3 for examples of power spectra.

**Table 1** Seismic velocities, densities and magnetic parameters. P-wave velocities ($V_p$) have been obtained from wells and OBS lines (e.g., Mjelde *et al.* (2005), see Osmundsen and Ebbing (2008) for more details), densities from velocity-density relations with an error in the order of ± 0.05 Mg/m$^3$ and ± 0.1 Mg/m$^3$ for the upper basement and the deep crustal layers, respectively. Magnetic susceptibility and Q-ratios have been transferred from onshore measurements. The inclination and declination of all remanent magnetic fields is set to 77.0° and 0.5°, approximately parallel to the present magnetic field. LCB: lower crustal body

| | $V_p$ (m/s) | Density (Mg/m$^3$) | Magnetic susceptibility (SI) | Q-ratio |
|---|---|---|---|---|
| Seawater | 1450 | 1.03 | 0 | 0 |
| Cenozoic sediments | 1800–2400 | 2.05–2.1 | 0.0001 | 0.4 |
| Upper Cretaceous sediments | 2400–3600 | 2.3–2.4 | 0.0002–0.003 | 0.4 |
| Lower Cretaceous sediments | 2800–5000 | 2.45–2.55 | 0.0002–0.003 | 0.4 |
| Jurassic sediments | 3200–3750 | | | |
| Triassic sediments | 4250–5000 | 2.65–2.7 | 0.0002–0.003 | 0.4 |
| Palaeozoic sediments | 5000–6000 | | | |
| Upper Caledonian basement | | 2.65–2.7 | 0.005–0.01 | 0.5–1.0 |
| Lower Precambrian basement | 6000–6500 | 2.75–2.85 | 0.02–0.035 | 0.4–1.1 |
| Lower crust | | 2.95–3.0 | 0.005 | 0.5 |
| LCB | 7000– | 3.1 | 0.005–0.0075 | 0.5 |
| Mantle | >8000 | 3.3 | 0.0025 | 0.5 |

source distance for magnetic anomalies also leads to a stronger dependency on upper crustal sources. Simplified, one can say that the magnetic field is mainly dependent on shallow crustal sources, while the Bouguer gravity field is caused by the density distribution and thickness of the entire crust.

In general, the gravity field of the mid-Norwegian margin does not include a prominent signal of the top basement because only a small density contrast exists between the sediments and the basement (Table 1, Fig. 5). This is due to the fact that in 10 km depth, the typical depth range for the top basement on the mid-Norwegian margin, sediments enter into greenschist facies and consequently lose porosity. Hence, determination of the top basement geometry mainly depends on the magnetic interpretation.

For the 3D modelling, we use the Interactive Gravity and Magnetic Application System (IGMAS), which calculates the potential field effect of the model by triangulating between parallel, vertical planes (Götze and Lahmeyer 1988). The 3D

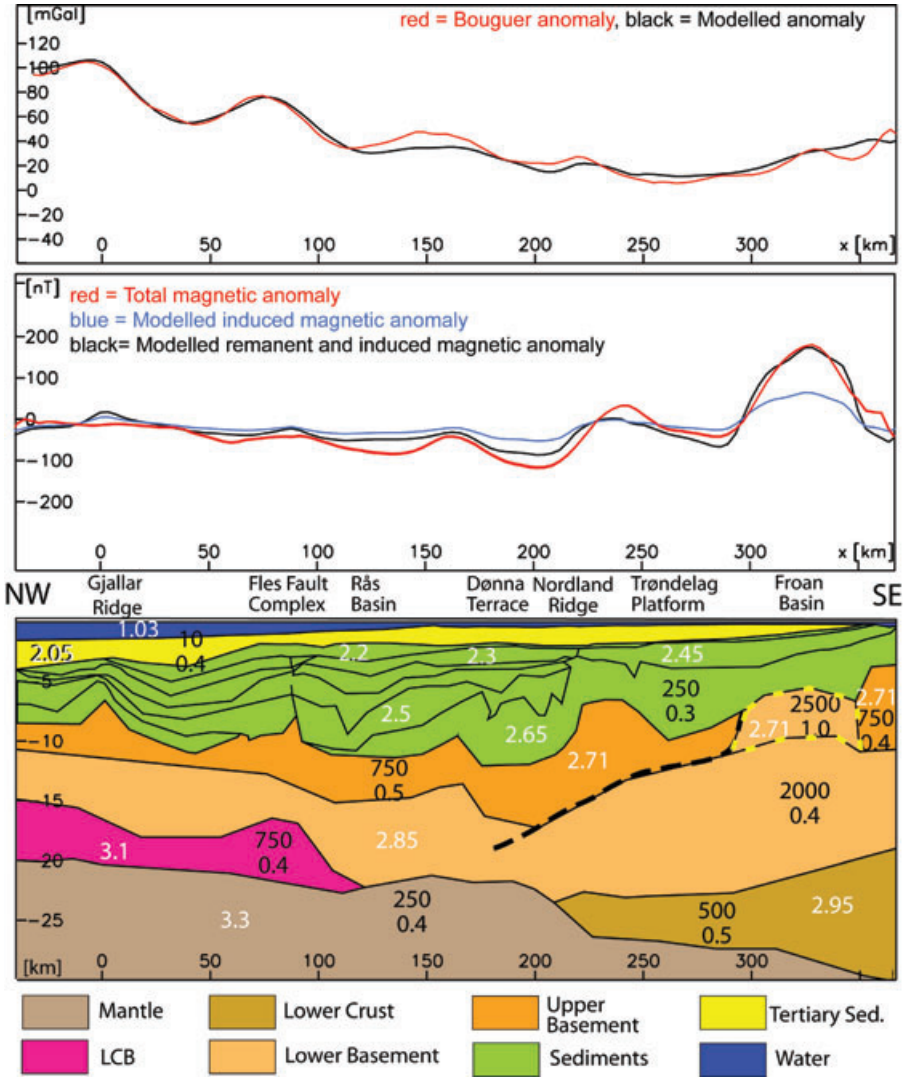


**Figure 5** Profile through the 3D model (see Fig. 1 for location). The upper panel shows the magnetic anomaly, the middle panel the gravity anomaly. The lower panel shows the modelled cross-section. White numbers are density values in $Mg/m^3$; black numbers show magnetic susceptibility ($10^{-5}$ SI) and Q-ratio. LCB: lower crustal body. The profile represents a typical transect through the mid-Norwegian margin and clearly illustrates the changes in gravity and magnetic anomalies as well as in crustal structure from the outer Vøring margin landwards towards the Trøndelag Platform. The bold, black dotted line indicates a basin-flank detachment and the yellow line the core complex below the Froan basin, as seen on seismic data (Osmundsen and Ebbing 2008).

model consists of 40 cross-sections with a spacing of 10–25 kilometres. This spacing provides coverage of the main large-scale geological features and a good overlay with the OBS and seismic reflection profiles (Fig. 1).

The most important parameters in the construction of the 3D model are the crustal geometry and the petrophysical properties (density, magnetic susceptibility and Q-ratio) for crust and upper mantle. The geometry of the 3D model is based on the studies mentioned above. These studies constrained the internal geometries of the sedimentary succession and crustal structure (e.g., rotated fault blocks). The densities for the model can be estimated from seismic velocities and borehole data (Table 1, Ebbing *et al.* 2006; Osmundsen and Ebbing 2008). The information about the susceptibility of the basement (Table 1) has, however, to be transferred from petrophysical studies onshore. Studies by Olesen *et al.* (1991), Skilbrei, Skyseth and Olesen (1991) and Mørk, McEnroe and Olesen (2002) showed that the susceptibilities of the basement can range between 0.005–0.035 SI while the susceptibilities of the overlying sediments are only in the order of 0.0003 SI,

some one- to two-orders of magnitude lower (Table 1). Hence, the contribution of the sediments to the magnetic field is only small and the main sources can be expected to reside within basement rocks and intra-sedimentary volcanic rocks. Intra-sedimentary rocks are mainly expected close to the marginal high and to be expressed by low-wavelength magnetic anomalies and not addressed in detail in our regional model.

Petrophysical studies of rocks exposed in onshore areas that flank the mid-Norway margin show that we can differentiate between two types of basement: a high-magnetic part corresponding to Precambrian granulite facies rocks and a low-magnetic part corresponding to Caledonian nappes and amphibolite facies Precambrian basement (Olesen *et al.* 1991; Skilbrei *et al.* 1991). We will refer to these units as lower (Precambrian) and upper (Caledonian) basement units, respectively. The direction of the remnant magnetization is modelled to be parallel to the present magnetic field, as observed for high-grade rocks in Lofoten (Olesen *et al.* 1991) and on the Fosen Peninsula (Skilbrei *et al.* 1991). The inclination and declination of all remnant fields is set to 77.0° and 0.5°, approximately parallel to the present Earth magnetic field.

Onshore-offshore correlations allow us to attribute magnetic properties to the basement rocks. As shown later, high-magnetic basement rocks at shallow crustal levels are related to prominent gravity and magnetic anomalies, especially below the Trøndelag Platform. Joining the interpretation of magnetic and seismic data these magnetic basement units can be traced in depth and from the Trøndelag Platform below the Vøring Basin (Osmundsen and Ebbing 2008).

## Modelling results

The final 3D model of the mid-Norwegian margin has a standard deviation of <7.5 mGal between the observed and modelled gravity field and <90 nT between the magnetic fields. The error for the gravity field is in the order of the error in marine gravity data (Skilbrei *et al.* 2000). The error in the magnetic field is mainly related to short-wavelength, high-amplitude anomalies at the continent-ocean and onshore-offshore transition and to the resolution of the 3D model. The amount of constraints used in constructing the 3D model leads to an overall accuracy of the depth horizons within ±5% depending on the reliability of the regional seismic data. For the intra-basement structures the depth error can be higher due to small density and velocity contrasts and due to the uncertainties in the velocities used in the depth conversion. The overall geometry is, however, fairly well constrained by the seismic reflection data.

Figure 5 shows a cross-section through the 3D model. The transect is crossing the central part of the margin from the outer Vøring Basin through the Rås Basin and Halten Terrace into the Trøndelag Platform. This transect illustrates the main characteristics of the crustal structure of the mid-Norwegian margin: very thick sedimentary sequences divided by major boundary faults; a thin upper basement underlain by a high-magnetic basement, locally cutting through the upper basement; low-amplitude magnetic anomalies on the outer Vøring margin but high-amplitude magnetic anomalies on the Trøndelag Platform; core complexes associated with high magnetic anomalies; a thick high-density lower crustal body on the outer Vøring margin; a flat Moho geometry, rapidly deepening landwards below the Trøndelag Platform. Most of the structures are associated with large density contrasts. Only a small density contrast (0.05–0.1 Mg/m$^3$) occurs between the upper and lower basement, the magnetic contrast is however significant. On the profile (Fig. 5) a crustal dome (core complex) can be clearly seen. On the magnetic anomaly map (Fig. 2) the magnetic high of the Frøya High clearly extends into the southern Halten Terrace.

The profile shows that the influence of the high-magnetic lower basement on the magnetic signal of the outer Vøring margin is relatively small due to the flat-lying boundary between the upper and lower basement and its large depth. In some areas west of the Vigra High and in the areas of flat basement, sediments also appear to be juxtaposed with the lower basement across extensional 'basin floor'-detachment faults. The division of the basement in the upper low-magnetic basement and the lower high-magnetic basement explains the different characteristics of the magnetic anomalies on the mid-Norwegian margin without the need to introduce the Curie temperature depth at shallow crustal depths or with a high thermal gradient.

In the 3D model, the layers below the lower basement feature a non-zero magnetization. These layers only give a minor contribution to the individual magnetic anomalies but increase the adjustment for the long-wavelength, regional anomaly pattern of the 3D model. Note that the deepest sources are in contradiction with the depth estimates from the spectral methods.

The 3D model also allows us to extract maps of the upper and lower basement, the base of the crust (Moho) and the continental lower crust and the lower crustal body ($V_p$ > 7km/s). The interpretation of these horizons is mainly based on the OBS profiles and the density modelling, as the deep part of the crust has only a minor influence on the magnetic field due to the large distance to the source. A discussion of the deep

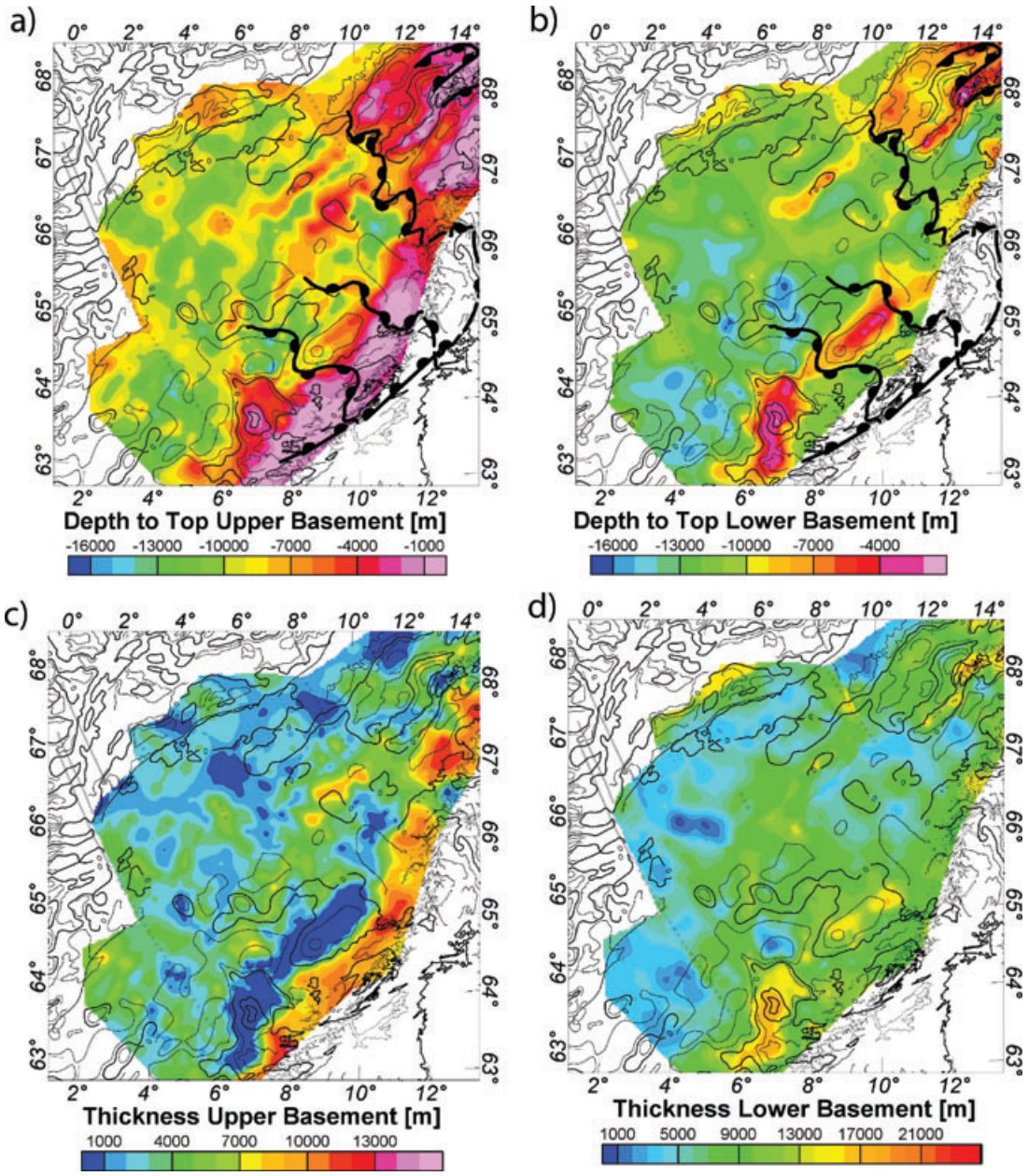


**Figure 6** Depth and thickness of upper (Caledonian) and lower (Precambrian) basement. a) The depth to the top lower basement is associated with the depth to the top of the Caledonian nappes with densities around 2.7 Mg/m$^3$ and relatively low susceptibilities compared to the underlying Precambrian basement. b) Depth to the lower (Precambrian) basement defined by densities >2.75 Mg/m$^3$ and higher magnetic properties compared to the upper basement. c) Thickness of upper basement. d) Thickness of lower basement defined by Precambrian basement and above layers with densities >3.0 Mg/m$^3$ (~velocities > 7 km/s; e.g., LCB; mantle). The lateral extend of the maps is given by the extent of the 3D density model. Contour lines show the total magnetic field anomaly as overlay (contour distance 100 nT).

crustal geometry and the meaning of the lower crustal density distribution can be found in Ebbing *et al.* (2006). Here, we focus on the basement composition and the magnetic anomalies.

### Basement configuration

The map of the top (Caledonian) basement (Fig. 6) reveals a deepening from the coastal area towards the continental

margin. Below the Trøndelag Platform the top basement is located at depths between 3 and 10 km, while in the Vøring Basin, the top basement is generally encountered between 11 and 15 km. Our map of the top basement shows a variety of local features, such as basement highs that correlate with the Nyk and Utgard Highs, which also reveal positive gravity anomalies. The depth to the top basement is also reflecting basement highs, which are not present in the southern Vøring Basin. North-east of the Bivrost Lineament the top of the crystalline basement is located at a depth less than 10 km and locally reaches the surface at the Lofoten Ridge.

The lower (Precambrian) basement is a key element in the potential field that signals on the mid-Norwegian margin and can be directly associated with potential field anomalies on the Trøndelag Platform. The lower basement is defined to have densities >2.75 Mg/m$^3$ and higher magnetic properties than the uppermost basement (see Table 1). The top lower basement is generally located at depths >12 km and on the Trøndelag Platform it defines extended structural highs at depths <3 km. These highs are aligned and can appear to be a continuous high from the Frøya High along the western border of the Froan basin. However, the Frøya High is very broad and terminates in the north by the offshore prolongation of the late-Caledonian Høybakken detachment (see Fig. 2 in Ebbing *et al.* 2006). The geometry of the lower (Precambrian) basement can be identified in detail in a wide-angle reflection line of the area (Osmundsen and Ebbing 2008). The comparison with the magnetic field anomaly shows that the top of the lower basement correlates directly with the magnetic anomalies for the Frøya High and the shape of the main magnetic lows. The area of the low-magnetic anomalies on the outer Vøring margin is in general associated with a depth to the top lower basement of more than 12 km.

Mapping of the different crustal horizons allows us also to calculate the thickness of the basement and here we present the thickness of the upper and lower basement separately. The upper basement has generally a thickness of only 1–3 km on the outer Vøring margin. On the Trøndelag Platform the upper (Caledonian) basement is thinning out in the areas of the core complexes, where the lower (Precambrian) basement underlies directly the sedimentary successions. A similar situation is encountered under the deepest parts of the basins in association with the basin-floor detachments. The thickness of the lower basement is calculated from the top of the lower basement to the layer with seismic P-velocities >7 km/s (e.g., Moho, lower crustal body). The resulting thickness of the lower basement is also showing a thinning towards the outer margin from 7–12 km below the Trøndelag Platform to less than 6 km below the outer Vøring margin. The lower basement thickness is also correlated surprisingly well with the shape of the magnetic anomaly. The magnetic high associated with the Frøya High is an effect of a very shallow and thick lower high-magnetic basement. The thickness below the Vøring Basin is significantly reduced and the magnetic anomaly field is relatively low amplitude. Consequently, our analysis allows us to argue that the relatively low-amplitude magnetic anomalies on the outer Vøring Basin could be mainly related to the thinning and deepening of high-magnetic material in the lower basement. These results indicate a strong relation between thickness and depth of the lower basement and the magnetic signal of the mid-Norwegian margin. In the next step, we model the thermal structure along a profile to evaluate the possibility of shallow Curie isotherms in more detail.

**Table 2** Parameters used in the thermal modelling

| Layer | $k$ (W/m/K) | $A_0$ ($\mu$W/m$^3$) |
|---|---|---|
| Cenozoic sediments | 1.5 | 0.5 |
| Other sediments* | 2.0 | 0.5 |
| Upper basement | 2.5 | 1.5 |
| Lower basement | 2.5 | 0.1 |
| Lower crust and LCB | 3 | 0.1 |
| Mantle | 3.5 | 0 |

## THERMAL MODELLING

We carried out 2D thermal modelling, by means of finite element methods, in order to test the reliability of the Curie depths as deduced from the spectral analysis of the magnetic field (Fig. 4). Selected parameters and the adopted geometry for the modelled profile are given in Table 2 and in Fig. 5 respectively. Heat generation values were attributed assuming that the low-magnetic basement corresponds to Caledonian nappes whereas the high-magnetic basement is the Precambrian substratum as suggested by onshore petrophysical measurements (Slagstad 2008). Typical thermal conductivity values are inferred for the different layers of the model (Table 2). Noteworthy the results presented below are not very sensitive to the uncertainties commonly attached to thermal conductivity values. Temperatures and horizontal heat flow are set equal to zero at the surface and the lateral edges of the model, respectively.

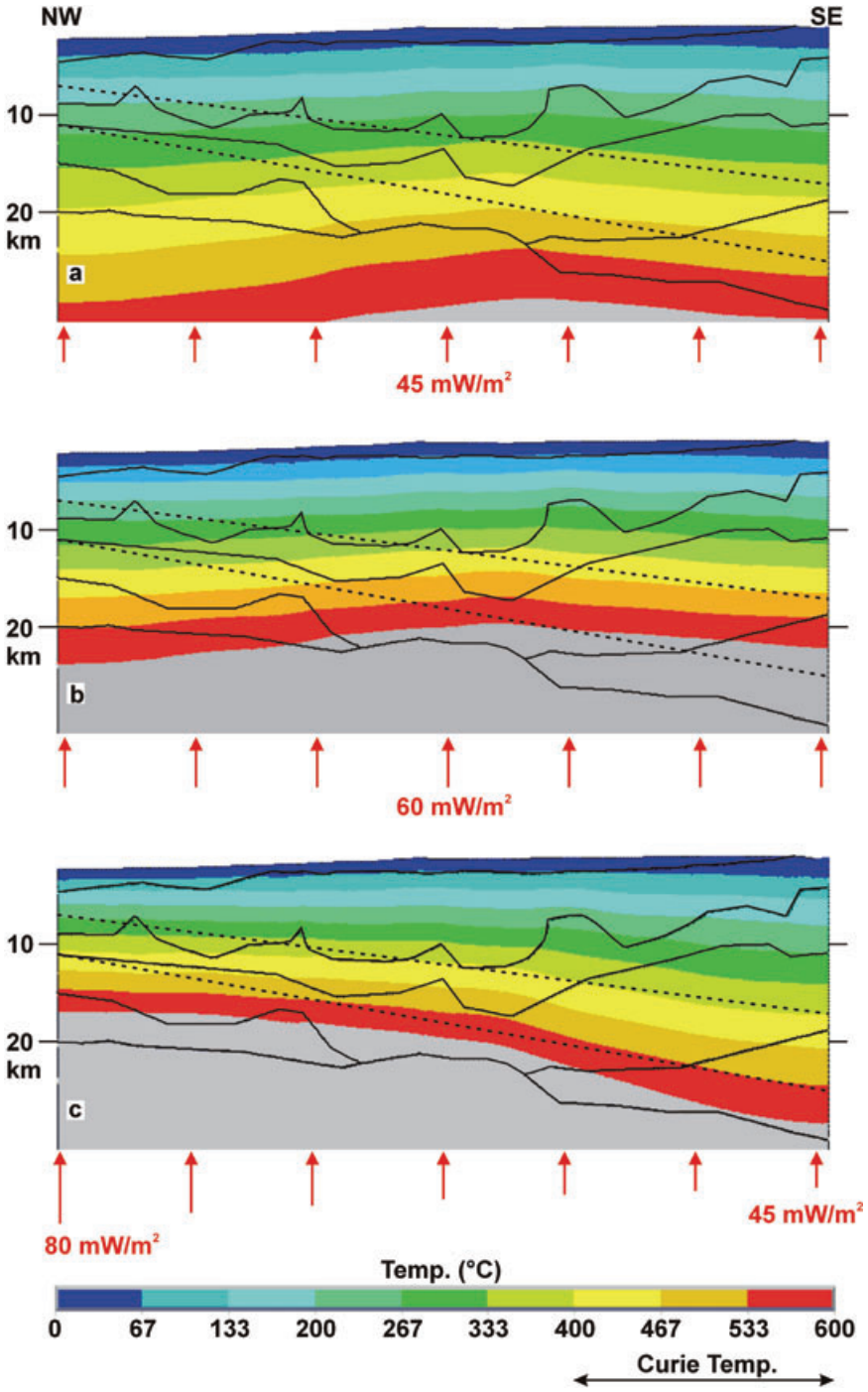


**Figure 7** Modelled isotherms in function of basal heat flow. Dashed lines represent the uppermost and lowermost estimates for Curie depths as derived from the spectral analysis (Figs 3 and 4). Model parameters are given in Table 2.

We made different modelling tests by varying basal heat flow values. Relevant modelling results for the present discussion are shown in Fig. 7 together with the upper and lower boundaries for Curie temperatures as determined from the spectral analysis. For the first modelling case (Fig. 7a), basal heat flow is set constant to 45 mW/m$^2$. Near the eastern boundary of the model (i.e., close to the Norwegian coastline) we found a reasonable fit between the range of depths to the

Curie temperatures estimated from the spectral analysis and the modelled depths for the 400° and 600°C isotherms. However, from the central part of the model to its western boundary (i.e., ocean-continent transition), predicted temperatures drop quickly well below 400°C for the specific Curie depth range suggested by the spectral analysis. Increasing the basal heat flow to 60 mW/m$^2$ (Fig. 7b) does not notably improve the fit at the western edge of the model and this latter value appears to be somehow excessive at its eastern edge. Alternatively, basal heat flow can be assumed to increase gradually from the coastline to the ocean-continent transition, reflecting the transition from the old and cold stable craton to the relatively young (i.e., up to 65–54 Ma) oceanic lithosphere. Figure 7(c) presents predicted isotherms for a basal heat flow increasing westwards from 45–80 mW/m$^2$. The thermal pattern mimics what is very often assumed in the literature (e.g., Fichler *et al.* 1999) and reasonably fits our previously estimated Curie depths, except at the ocean-continent transition where the 400°C isotherm hardly meets their lowermost boundary. This last result calls for a further increase of the applied basal heat flow below the ocean-continent transition (i.e., more than 80 mW/m$^2$) in order to get modelled temperatures in the range of 400°–600°C at the depths predicted for the Curie temperatures by the spectral analysis. An alternative could be to increase modelled heat generation values in the lower crust. However, even an increase of heat generation rates to 0.5 mW/m$^3$, would result in a negligible upwelling of the isotherms. Such a value represents a higher bound for lower crustal rocks, especially if they are considered mafic, as suggested by the high seismic P-velocities values (e.g., Mjelde *et al.* 2005).

Finally, we compared our modelled surface heat flow values with published data (Fig. 8). Although much care has to be taken here, especially with marine heat flow data when collected at relatively shallow water depths (see discussion in Ritter *et al.* 2004), surface heat flow seems to increase oceanwards from the centre of the study area. Heat flow values predicted by model A are in reasonable agreement with data in the eastern to the central part of the margin but seem to underestimate measured values near the ocean-continent transition. Nevertheless, the main and clear result from this modelling exercise is that model C, the most satisfactory one in terms of fitting Curie temperature depths as determined from spectral analysis, clearly overestimates by 15 to more than 20 mW/m$^2$ measured heat flow values. In brief, near the coastline Curie depths estimated by spectral analysis can reasonably be correlated to crustal temperatures ranging from 400°–600°C but at the ocean-continent transition, the modelling and the data at hand demonstrate that the determined depth estimates from the spectral method do not reflect the thermal state of the crust.

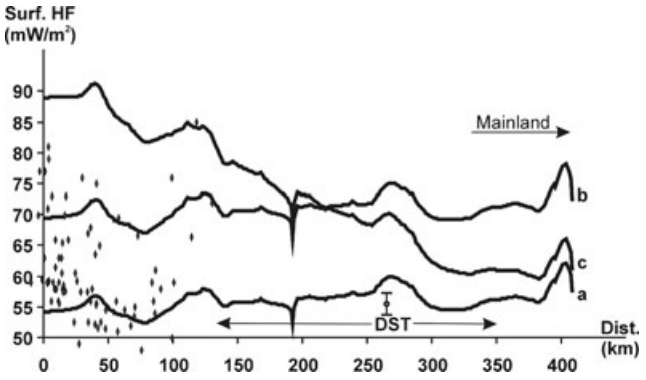


**Figure 8** Modelled surface heat flow. a), b) and c) correspond to model cases depicted in Fig. 7. Diamonds represent marine heat flow measurements from Haenel (1974), Sundvor *et al.* (1989) and Ritter *et al.* (2004) projected on the modelled line. Mean heat flow and its associated standard deviation from borehole temperature data (DST) are from Ritter *et al.* (2004), the arrows show the approximate spatial coverage of the wells.

## DISCUSSION

The thermal model in Fig. 7 shows along a transect the geometry of the 3D model and the spectral estimates for the deepest magnetic source. Along this transect the depth estimates for the bottom of the magnetic sources are around 10 km in the oceanic domain and 18 km depth in the continental domain (Fig. 4). These depth estimates are located in the lower crust and show an apparent correlation with the boundary between the lower (Precambrian) basement and the underlying lower crust below the Trøndelag Platform and between the upper and lower basement on the outer Vøring margin. A correlation between depth to the bottom of magnetic sources and modelled isotherms appears near the Norwegian coastline but this good fit is difficult to obtain at the ocean-continent transition as previously suggested by Gernigon *et al.* (2006). On the oceanic domain the depth solutions are not modelled in any detail but should be in the range of 20–30 km depth according to plate cooling models (e.g., Stein and Stein 1992).

Our interpretation shows that the main magnetic signature of the mid-Norwegian margin is related to the changing geometry of the basement. Consequently, the bottom of the magnetic sources may be mostly controlled by the structure of the margin instead of its thermal state. We further suggest that the Curie temperature depths cannot easily be derived

from magnetic data along mature continental passive margins. One further uncertainty is inherited in the method of power spectrum estimates of depth to magnetic sources. Different variations of the power spectrum method exist (e.g., Shuey *et al.* 1977; Connard *et al.* 1983; Okubo *et al.* 1985; Fedi *et al.* 1997; Aydin *et al.* 2005; Ross *et al.* 2006) and the application to a complex geological situation is not straightforward.

We applied the method after Okubo *et al.* (1985), even though our results raise some doubts about the validity of its application to the mid-Norwegian margin. In the spectra (Fig. 3) it is difficult to observe peaks and the results depend largely on the window size. Clearly, very large windows must be used to be able to estimate the bottom of magnetic sources. The changes in the depth estimates with different window sizes (Fig. 4) may indicate that the window size was not large enough to resolve the deepest magnetic sources. Even more challenging is however, that with such large window sizes averages over magnetic sources and different tectonic settings are made. All these pitfalls in the application of the spectral method increase the uncertainty of the results. Using only depth estimates from the power spectrum method, it is certainly difficult to distinguish between thermal and structural control of the deepest magnetic sources.

Another important point is the implication of our study for the thermal state of the mid-Norwegian margin. Fichler *et al.* (1999) explained in their favourite model the observed discrepancy between the gravity and magnetic patterns by a high thermal gradient. They assumed that thermal gradients of 30°C/km and 50°C/km are typical for the continental shelf and the oceanic crust, respectively, placing the Curie isotherms at depths of around 20 km and 11 km (i.e., using 580°C as Curie temperature). These assumptions look to be much too crude and even erroneous in the case of old oceanic crust for putting physical grounds to any interpretation of Curie temperature depths. Although the first assumed gradient value appears to be an acceptable first-order estimate for the mid-Norwegian margin, at least as long as the sedimentary cover is concerned, it should not be extrapolated to the underlying basement (simply because of contrasting thermal conductivities between porous sediments and crystalline basement). Gernigon *et al.* (2006) mentioned this inaccuracy and modelled the thermal structure along the Vøring margin. They obtained a far lower thermal gradient, which places the Curie isotherms in the lower crust or upper mantle. Concerning the assumed gradient value for oceanic crust, it implies a surface heat flow of ~150 mW/m$^2$ (assuming a thermal conductivity of 3 W/m/K for the mafic oceanic basement) at odds with marine heat flow data collected in the oceanic basins adjacent to the mid-Norwegian margin (i.e., ~60 mW/m$^2$; Sundvor *et al.* 2000). Furthermore, in the resulting model, the magnetic data covering the Vøring Basin reflect only the topography of the basement and intra-crustal inhomogeneities within the upper crust, because the lower boundary of the magnetic crust, i.e., the Curie isotherm of 580°C, is at a depth of approximately 20 km beneath the Halten Terrace and at a depth of 13 km in the western Vøring Plateau (Fichler *et al.* 1999). This restricts the magnetic sources to the uppermost part of the basement as the depths to the top of the basement are close to the depths of the Curie isotherm. Consequently, this would explain the low-magnetic amplitudes.

Applying a 'lower' but certainly more realistic thermal gradient, (i.e., that would place the depth to the Curie isotherms in the lower crust or upper mantle) a model featuring a distinct boundary between the upper and lower basement can easily explain the observed potential field signatures. In our interpretation, the lower high-magnetic basement is losing its influence on the magnetic field solely by the increased depth and the flat-lying contrast to the upper basement, due to the high dependency of the magnetic field to the source distance. This interpretation appears to be reasonable, even if the confidence in the depth estimates of the boundary is less than for the upper basement due to the large variability of magnetic properties and the small density contrast at the boundary.

With increasing depth, the influence of the lower (Precambrian) basement on the magnetic anomalies decreases. Furthermore, the contact between the upper and lower basement becomes flat on the outer Vøring margin but can be traced below the Trøndelag Platform where it culminates in the core complexes. These core complexes cause the most prominent anomalies on the mid-Norwegian margin and their distribution is controlled by the late-Caledonian bounding detachments, which can be linked from onshore Norway (Olesen *et al.* 2002; Ebbing *et al.* 2006). Along the platform boundaries, the normal configuration of the lower basement can be observed, with the superposition of Mesozoic structures on the late-Caledonian configuration (Osmundsen and Ebbing 2008).

The ambiguity in potential field modelling leaves the possibility of a change in Curie temperature depth along the margin. However, our thermal modelling showed that a high thermal gradient would be expressed by a much larger surface heat flow than measured (Sundvor, Myhre and Eldholm 1989; Ritter *et al.* 2004). Comparison between structural and thermal modelling confirms our interpretation that the observed magnetic field on the mid-Norwegian margin does not

reflect the Curie temperature depth as previously assumed but mostly the geometry of the basement and lower crust. Further evidence against a high thermal gradient comes from thermal modelling based on structural models of the margin.

## CONCLUSION

Depth estimates by spectral methods indicate a shallowing of deepest magnetic sources from the Norwegian coast towards the outer Vøring margin, although depth estimates have large uncertainties due to complexity of the geology on the mid-Norwegian margin and pitfalls associated to the spectral method. Thermal modelling assuming a high thermal gradient, under the assumption that spectral estimates represent the Curie isotherms, leads to unreasonable surface heat flow values on the outer Vøring margin. The combined interpretation of gravity and magnetic allows us to identify the crustal structure on the Norwegian passive margin. In combination with seismic data potential field models can be used to identify the top of the basement, even at large depths, as well as the deep crustal configuration. The integrated interpretation of all the different methods presented in this study, makes us conclude that the relatively magnetic quietness on the outer Vøring margin is mainly related to the deep and thin, high-magnetic lower 'Precambrian' basement. The 3D model shows that the lower basement is a key source for the potential field signals on the mid-Norwegian margin and especially on the Trøndelag Platform. The changes in the magnetic anomaly pattern from the Trøndelag Platform to the Vøring Basins and the discrepancy between gravity and magnetic anomaly patterns on the outer Vøring margin are likely to have a structural and not a thermal explanation.

## ACKNOWLEDGEMENTS

The study is done as part of the project KONTIKI (Continental Crust and Heat Generation in 3D) supported by StatoilHydro. We express our gratitude to all our industrial partners and more specifically to Øyvind Steen. We are indebted to Rolf Mjelde and Thomas Raum for permission to use unpublished interpretations of OBS data in the upgrading of our 3D density model and in the depth conversion of seismic lines. Discussions with Christine Fichler (StatoilHydro) are greatly appreciated. We thank also Claudia Haase for assistance during the spectral estimates, Claire Bouligand, Rick Blakely and Angelo DeSantis for their constructive comments on the manuscript and TGS-NOPEC Geophysical Company for permission to use the magnetic data on the Møre and Vøring margin.

## REFERENCES

Åm K. 1975. Aeromagnetic basement complex mapping north of latitude 62°N, Norway. *Norges Geologiske Undersøkelse* **316**, 351–374.

Andersen O.B. and Knudsen P. 1998. *Gravity anomalies derived from the ERS-1 satellite altimetry*. Kort og Martykelstyrelsen, Kopenhagen.

Artemieva I.M. and Mooney W.D. 2001. Thermal thickness and evolution of Precambrian lithosphere: A global study. *Journal of Geophysical Research* **106**, 16387–16414.

Aydın I., Karat H.I. and Koçak A. 2005. Curie-point depth map of Turkey. *Geophysical Journal International*, **162**, 633–640.

Beardsmore G.R. and Cull J.P. 2001. *Crustal Heat Flow – A Guide to Measurements and Modelling*. Cambridge University Press.

Bhattacharyya B. 1964. Magnetic anomalies due to prism-shaped bodies with arbitrary polarization. *Geophysics* **29**, 517–530.

Blakely R. 1996. *Potential Theory in Gravity and Magnetic Applications*. Cambridge University Press.

Blystad P., Brekke H., Færseth R.B., Larsen B.T. Skogseid J. and Tørudbakken B. 1995. *Structural elements of the Norwegian continental shelf, Part II. The Norwegian Sea Region*. Norwegian Petroleum Directorate Bulletin 8.

Brekke H. 2000. The tectonic evolution of the Norwegian Sea continental margin with emphasis on the Vøring and Møre basins. In: *Dynamics of the Norwegian Margin* (ed. A. Nøttvedt), pp. 327–378. Geological Society of London.

Byerly P. and Stolt R. 1977. An attempt to define the Curie point isotherm in northern and central Arizona. *Geophysics* **42**, 1394–1400.

Connard G., Couch R. and Gemperle M. 1983. Analysis of aeromagnetic measurements from the Cascade Range in central Oregon. *Geophysics* **48**, 376–390.

Dehls J.F., Olesen O., Bungum H., Hicks E., Lindholm C.D. and Riis F. 2000. *Neotectonic Map, Norway and Adjacent Areas 1:3 Mill*. Norges Geologiske Undersøkelse, Trondheim, Norway.

Doré A.G., Lundin E.R., Jensen L.N., Birkeland Ø., Eliassen P.E. and Fichler C. 1999. Principal tectonic events in the evolution of the northwest European Atlantic margin. In: *Petroleum Geology of Northwest Europe: Proceedings of the 5th Conference* (eds A.J. Fleet and S.A.R. Boldy), pp. 41–61. Geological Society of London.

Ebbing J., Lundin E., Olesen O. and Hansen E.K. 2006. The mid-Norwegian margin: A discussion of crustal lineaments, mafic intrusions, and remnants of the Caledonian root by 3D density modelling and structural interpretation. *Journal of the Geological Society, London* **163**, 47–60.

Fedi M., Quarta T. and De Santis A. 1997. Inherent power-law behavior of magnetic field power spectra from a Spector and Grant ensemble. *Geophysics* **62**, 1143–1150.

Fichler C., Rundhovde E., Olesen O., Sæther B.M., Rueslåtten H., Lundin E. et al. 1999. Regional tectonic interpretation of image

enhanced gravity and magnetic data covering the Mid-Norwegian shelf and adjacent mainland. *Tectonophysics* **306**, 183–197.

Fowler C.M.R. 2005. *The Solid Earth – An Introduction To Global Geophysics*, 2nd edn. Cambridge University Press.

Gernigon L., Lucazeau F., Brigaud F., Ringenbach J. C. and Le Gall B. 2006. A moderate melting model for the Vøring margin (Norway) based on structural observations and a thermo-kinematical modelling: Implication for the meaning of the lower crustal bodies. *Tectonophysics* **412**, 255–278.

Gernigon L., Olesen O., Ebbing J., Wienecke S., Gaina C., Mogaard J.O.*et al*. 2009. Geophysical insights and early spreading history in the vicinity of the Jan Mayen Fracture Zone, Norwegian-Greenland Sea. *Tectonophysics* (in press).

Gernigon L., Ringenbach J.-C., Planke S. and Le Gall B. 2004. Deep structure and breakup along volcanic rifted margins: insights from integrated studies along the outer Vøring Basin (Norway). *Marine and Petroleum Geology* **21**, 363–372.

Götze H.-J. and Lahmeyer B. 1988. Application of three-dimensional interactive modeling in gravity and magnetics. *Geophysics* **53**, 1096–1108.

Haenel R. 1974. Heat flow measurements in the Norwegian Sea. *Meteor-Forschungsergebnisse Reihe C: Geologie und Geophysik* **17**, 74–78.

Hunt C.P., Moskowitz B.M. and Banerjee S.K. 1995. Magnetic properties of rocks and minerals. In: *Rock Physics and Phase Relations. A Handbook of Physical Constants* (ed. T.J. Ahrens), pp. 189–204. American Geophysical Union.

Kukkonen I.T. and Peltonen P. 1999. Xenolith-controlled geotherms for the central Fennoscandian Shield: Implications for lithosphere-asthenosphere relations. *Tectonophysics* **304**, 301–315.

Maus S., Gordon D. and Fairhead J.D. 1997. Curie-temperature depth estimation using a self-similar magnetization model. *Geophysical Journal International* **129**, 163–168.

McKenzie D., Jackson J. and Priestley K. 2005. Thermal structure of oceanic and continental lithosphere. *Earth and Planetary Science Letters* **233**, 337–349.

Mjelde R., Digranes P., van Schaack M., Shimamura H., Shiobara H., Kodaira S.*et al*. 2001. Crustal structure of the outer Vøring Plateau, offshore Norway, from ocean bottom seismic and gravity data. *Journal of Geophysical Research* **106**, 6769–6791.

Mjelde R., Faleide J.I., Breivik A.J. and Raum T. 2009. Lower crustal composition and crustal lineaments on the Vøring Margin, NE Atlantic: A review. *Tectonophysics* (in press).

Mjelde R., Raum T., Breivik A., Shimamura H., Mural Y., Takanami T.*et al*. 2005. Crustal structure of the Vøring margin, NE Atlantic: A review of geological implications based on recent OBS data. In: *Petroleum Geology: North-West Europe and Global Perspectives – Proceedings of the 6th Petroleum Geology Conference* (eds A.G. Doré and B.A. Vining), pp. 803–813. Geological Society of London.

Mjelde R., Raum T., Digranes P., Shimamura H., Shiobara H. and Kodaira S. 2003a. $V_p/V_s$ ratio along the Vøring Margin, NE Atlantic, derived from OBS data: Implications on lithology and stress field. *Tectonophysics* **369**, 175–197.

Mjelde R., Shimamura H., Kanazawa T., Kodaira S., Raum T. and Shiobara H. 2003b. Crustal lineaments, distribution of lower crustal intrusives and structural evolution of the Vøring Margin, NE Atlantic; New insight from wide-angle seismic models. *Tectonophysics* **369**, 199–218.

Mørk M.B.E., McEnroe S.A. and Olesen O. 2002. Magnetic susceptibility of Mesozoic and Cenozoic sediments off Mid Norway and the role of siderite: Implications for interpretation of high-resolution aeromagnetic anomalies. *Marine and Petroleum Geology* **19**, 1115–1126.

Nadeau P.H., Bjørkum P.A. and Walderhaug O. 2005. Petroleum system analysis: Impact of shale diagenesis on reservoir fluid pressure, hydrocarbon migration and biodegradation risks. In: *Petroleum Geology: North-West Europe and Global Perspectives – Proceedings of the 6th Petroleum Conference* (eds. A.G. Doré and B. Ving), pp. 1267–1274. Geological Society of London.

Naidu P. S. and Mathew M. P. 1998. Correlation filtering: A terrain correction method for aeromagnetic maps with application. *Journal of Applied Geophysics* **32**, 269–277.

Okubo Y., Graft R.J., Hansen R.O., Ogawas K. and Tsu H. 1985. Curie point depths of the Island of Kyushu and surrounding areas, Japan. *Geophysics* **53**, 481–494.

Olesen, O., Ebbing, J., Lundin, E., Mauring, E., Skilbrei, J.R., Torsvik, T.H.*et al*. 2007. An improved tectonic model for the Eocene opening of the Norwegian–Greenland Sea: Use of modern magnetic data. *Marine and Petroleum Geology* **24**, 53–66. doi:10.1016/j.marpetgeo.2006.10.008

Olesen O., Henkel H., Kaada K. and Tveten E. 1991. Petrophysical properties of a prograde amphibolite – granulite facies transition zone at Sigerfjord, Vesterålen, Northern Norway. *Tectonophysics* **192**, 33–39.

Olesen O., Lundin E., Nordgulen Ø., Osmundsen P.T., Skilbrei J.R., Smethurst M.A.*et al*. 2002. Bridging the gap between the onshore and offshore geology in Nordland, northern Norway. *Norwegian Journal of Geology* **82**, 243–262.

Osmundsen P.T. and Ebbing, J. 2008. Styles of extension offshore Mid Norway and implications for mechanisms of Late Jurassic-Early Cretaceous rifting. *Tectonics* **27**, TC6016. doi:10.1029/2007TC002242

Osmundsen P.T., Sommaruga A., Skilbrei J.R. and Olesen O. 2002. Deep structure of the Mid-Norway rifted margin. *Norwegian Journal of Geology* **82**, 205–224.

Pilkington M. and Todoeschuck J. P. 1993. Fractal magnetization of continental crust. *Geophysical Research Letters* **20**, 627–630.

Raum T., Mjelde R., Digranes P., Shimamura H., Shiobara H., Kodaira S.*et al*. 2002. Crustal structure of the southern part of the Vøring Basin, mid-Norway, from wide-angle seismic and gravity data. *Tectonophysics* **355**, 99–126.

Ritter U., Zielinski G.R., Weiss H.M., Zielinski R.L.B. and Sættem J. 2004. Heat flow in the Vøring Basin, Mid-Norwegian Shelf. *Petroleum Geoscience* **10**, 353–365.

Ross H.E., Blakely R.J. and Zoback M.D. 2006. Testing the use of aeromagnetic data for the determination of Curie depth in California. *Geophysics* **71**, 51–59.

Shuey R., Schlechinger D., Tripp A. and Alley L. 1977. Curie depth determination from aeromagnetic spectra. *Geophysical Journal of the Royal Astronomical Society* **50**, 75–102.

Skilbrei J.R., Kihle O., Olesen O., Gellein J., Sindre A., Solheim D.*et al*. 2000. *Gravity Anomaly Map Norway and Adjacent Ocean Areas, 1:3 Million*. Geological Survey of Norway (NGU), Trondheim.

Skilbrei J.R. and Olesen O. 2005. Deep structure of the Mid-Norwegian shelf and onshore-offshore correlations: Insight from potential field data. In: *Onshore-Offshore relationships on the North Atlantic Margin* (eds. B.T.G. Wandås, E.A. Eide, F. Gradstein and J.P. Nystuen), pp. 43–68. Norwegian Petroleum Society (NPF).

Skogseid J., Pedersen T., Eldholm O. and Larsen B.T. 1992. Tectonism and magmatism during NE Atlantic continental break-up: The Vøring margin. In: *Magmatism and the Causes of Continental Break-up* (eds B.C. Story, T. Alabaster and R.J. Plankhurst), pp. 305–320. Geological Society of London.

Skilbrei J.R., Skyseth T. and Olesen O. 1991. Petrophysical data and opaque mineralogy of high grade and retrogressed lithologies: Implications for the interpretation of aeromagnetic anomalies in northern Vestranden, Western Gneiss Region, Central Norway. *Tectonophysics* **192**, 21–31.

Slagstad T. 2008. Radiogenic heat production of Archean to Permian geological provinces in Norway. *Norwegian Journal of Geology* **88**, 149–166.

Spector A. and Grant F.S. 1970a. Application of high sensitivity aeromagnetic surveying to offshore petroleum exploration. *Geophysical Prospecting* **18**, 474–475.

Spector A. and Grant F.S. 1970b, Statistical models for interpreting aeromagnetic data. *Geophysics* **35**, 293–302.

Stein C.A. and Stein S. 1992. A model for the global variation in oceanic depth and heat flow with lithospheric age. *Nature* **359**, 123–129.

Sundvor E., Eldholm O., Gladczenko T. P. and Planke S. 2000. Norwegian-Greenland Sea thermal field. *Geological Society of London, Special Publications* **167**, 397–410.

Sundvor E., Myhre A. M. and Eldholm O. 1989. *Heat Flow Measurements on the Norwegian Continental Margin During the FLUNORGE Project*. Seismological Observatory, University of Bergen.

Tanaka A., Okubo Y. and Matsubayashi O. 1999. Curie point depth based on spectrum analysis of the magnetic anomaly data in East and Southeast Asia. *Tectonophysics* **306**, 461–470.

## APPENDIX

In complex geological settings, magnetic anomalies are caused by a large collection of magnetic sources with different shapes, depth and thickness. Following Spector and Grant (1970a) a simple statistical prism can be used to approximate an ensemble of magnetic sources. Estimates of the depth to the top and base of this prism provide information about the depths to the top and base of magnetic sources. The statistic prism is averaging over the individual magnetic sources from its top to base. Using gridded magnetic data, we can express the power density spectrum of the magnetic total field as a function of its magnetization $\Phi_{Mag}(k_x, k_y)$:

$$\Phi(k_x, k_y) = \Phi_{Mag}(k_x, k_y)F(k_x, k_y), \tag{1}$$

where the 2D Fourier transform $F(k_x, k_y)$ can also be expressed as (Blakely 1996):

$$F(k_x, k_y) = S^2_{(a,b)}(4\pi^2 C_m^2 M_d^2 G_d^2)e^{-2kz_{top}}(1 - e^{-k(z_{base}-z_{top})})^2, \tag{2}$$

with $S^2(a,b)$ the shape factor that is a function of the lateral shape of the statistical prisms, $M_d$ the factor associated to the magnetization direction and $G_d$ the factor associated to the geomagnetic field direction.

If we consider the radial average of the power density spectrum, this function can be simplified and approximated as:

$$\Phi_{average}(k) \sim e^{-2kz_{top}}(1 - e^{-k(z_{base}-z_{top})})^2, \tag{3}$$

This approximation requires that $\Phi_{\mathrm{mag}}(k_x, k_y)$ can be assumed to be constant, which is the case if the magnetization is random (Blakely 1996). We also assumed that $M_d$ and $G_d$ are constant. We may consider the logarithm of this equation:

$$\ln(\Phi_{average}(k)) \cong B - 2kz_{top} + 2\ln(1 - e^{-k(z_{base}-z_{top})}), \tag{4}$$

where $B$ is a constant.

At medium to high wavenumbers, the second term in this expression can be ignored, which leads to the following linear relationship:

$$\ln(\Phi_{average}(k)) \cong B - 2kz_{top}. \tag{5}$$

Therefore, the slope of $\ln(\Phi_{\mathrm{average}}(k))$ at medium to high wavenumbers can be used to estimate the depth to the top of a statistical prim.

Estimating the depth to the top of magnetic sources is more complicated. Equation (4) predicts that the radial power spectrum displays a peak at low wavenumbers. The precise location of this peak is related to the depth to the top and to the base of magnetic sources. The depth to the bottom of magnetic sources can therefore be estimated by locating this peak. However, such a peak is often difficult to observe in the power spectra (see Fig. 3a). Moreover, the superposition of the signals from different ensembles of magnetic sources further complicates the analysis.

Tanaka, Okubo and Matsubayashi (1999) and Okubo *et al.* (1985) proposed a different method to estimate the depth to the bottom of magnetic source. In this approach the depth to the bottom of the prism is estimated by equation (1) finding the depth to the top $z_{top}$ and equation (2) the depth to the

centroid $z_{centroid}$ of magnetic sources. The depth to the top of the prism is calculated from the slope of the radial power spectrum at high wavenumbers (equation (4)). Okubo *et al.* (1985) proposed that equation (4) can be approximated at low wavenumbers as follows:

$$\ln\left[\Phi_{average}(k)^{1/2}/k\right] \cong B - kz_{centroid}. \quad (6)$$

The depth to the centroid of the prism $z_{centroid}$, is therefore calculated from the slope of the radial power spectrum divided by the wavenumbers at low wavenumbers.

The depth to the base of the prism can be calculated from the depths to the top and centroid of the prisms, with:

$$z_{base} = 2z_{centroid} - z_{top}. \quad (7)$$